Title

A novel DPH5-related diphthamide-deficiency syndrome causing embryonic lethality or profound neurodevelopmental disorder

Journal

Genetics in Medicine, 24(7)

ISSN

1098-3600

Authors

Shankar, Suma P
Grimsrud, Kristin
Lanoue, Louise
et al.

Publication Date

2022-07-01

DOI

10.1016/j.gim.2022.03.014

Peer reviewed

HHS Public Access

Author manuscript

Genet Med. Author manuscript; available in PMC 2023 July 01.

Published in final edited form as:

Genet Med. 2022 July ; 24(7): 1567–1582. doi:10.1016/j.gim.2022.03.014.

*Correspondence and requests for materials should be addressed to Suma P. Shankar, XXX. spshankar@ucdavis.edu.

Members of the Undiagnosed Diseases Network

Maria T. Acosta, Margaret Adam, David R. Adams, Justin Alvey, Laura Amendola, Ashley Andrews, Euan A. Ashley, Mahshid S. Azamian, Carlos A. Bacino, Guney Bademci, Ashok Balasubramanyam, Dustin Baldridge, Jim Bale, Michael Bamshad, Deborah Barbouth, Pinar Bayrak-Toydemir, Anita Beck, Alan H. Beggs, Edward Behrens, Gill Bejerano, Jimmy Bennet, Beverly Berg-Rood, Jonathan A. Bernstein, Gerard T. Berry, Anna Bican, Stephanie Bivona, Elizabeth Blue, John Bohnsack, Devon Bonner, Lorenzo Botto, Brenna Boyd, Lauren C. Briere, Elly Brokamp, Gabrielle Brown, Elizabeth A. Burke, Lindsay C. Burrage, Manish J. Butte, Peter Byers, William E. Byrd, John Carey, Olveen Carrasquillo, Thomas Cassini, Ta Chen Peter Chang, Sirisak Chanprasert, Hsiao-Tuan Chao, Gary D. Clark, Terra R. Coakley, Laurel A. Cobban, Joy D. Cogan, Matthew Coggins, F. Sessions Cole, Heather A. Colley, Cynthia M. Cooper, Heidi Cope, William J. Craigen, Andrew B. Crouse, Michael Cunningham, Precilla D'Souza, Hongzheng Dai, Surendra Dasari, Joie Davis, Jyoti G. Dayal, Matthew Deardorff, Esteban C. Dell'Angelica, Katrina Dipple, Daniel Doherty, Naghmeh Dorrani, Argenia L. Doss, Emilie D. Douine, Laura Duncan, Dawn Earl, David J. Eckstein, Lisa T. Emrick, Christine M. Eng, Cecilia Esteves, Marni Falk, Liliana Fernandez, Elizabeth L. Fieg, Paul G. Fisher, Brent L. Fogel, Irman Forghani, William A. Gahl, Ian Glass, Bernadette Gochuico, Rena A. Godfrey, Katie Golden-Grant, Madison P. Goldrich, Alana Grajewski, Irma Gutierrez, Don Hadley, Sihoun Hahn, Rizwan Hamid, Kelly Hassey, Nichole Hayes, Frances High, Anne Hing, Fuki M. Hisama, Ingrid A. Holm, Jason Hom, Martha Horike-Pyne, Alden Huang, Yong Huang, Wendy Introne, Rosario Isasi, Kosuke Izumi, Fariha Jamal, Gail P. Jarvik, Jeffrey Jarvik, Suman Jayadev, Orpa Jean-Marie, Vaidehi Jobanputra, Lefkothea Karaviti, Jennifer Kennedy, Shamika Ketkar, Dana Kiley, Gonench Kilich, Shilpa N. Kobren, Isaac S. Kohane, Jennefer N. Kohler, Deborah Krakow, Donna M. Krasnewich, Elijah Kravets, Susan Korrick, Mary Koziura, Seema R. Lalani, Byron Lam, Christina Lam, Grace L. LaMoure, Brendan C. Lanpher, Ian R. Lanza, Kimberly LeBlanc, Brendan H. Lee, Roy Levitt, Richard A. Lewis, Pengfei Liu, Xue Zhong Liu, Nicola Longo, Sandra K. Loo, Joseph Loscalzo, Richard L. Maas, Ellen F. Macnamara, Calum A. MacRae, Valerie V. Maduro, Bryan C. Mak, May Christine V. Malicdan, Laura A. Mamounas, Teri A. Manolio, Rong Mao, Kenneth Maravilla, Ronit Marom, Gabor Marth, Beth A. Martin, Martin G. Martin, Julian A. Martínez-Agosto, Shruti Marwaha, Jacob McCauley, Allyn McConkie-Rosell, Alexa T. McCray, Elisabeth McGee, Heather Mefford, J. Lawrence Merritt, Matthew Might, Ghayda Mirzaa, Eva Morava, Paolo M. Moretti, Mariko Nakano-Okuno, Stan F. Nelson, John H. Newman, Sarah K. Nicholas, Deborah Nickerson, Shirley Nieves-Rodriguez, Donna Novacic, Devin Oglesbee, James P. Orengo, Laura Pace, Stephen Pak, J. Carl Pallais, Christina G.S. Palmer, Jeanette C. Papp, Neil H. Parker, John A. Phillips III, Jennifer E. Posey, Lorraine Potocki, Barbara N. Pusey, Aaron Quinlan, Wendy Raskind, Archana N. Raja, Deepak A. Rao, Anna Raper, Genecee Renteria, Chloe M. Reuter, Lynette Rives, Amy K. Robertson, Lance H. Rodan, Jill A. Rosenfeld, Natalie Rosenwasser, Francis Rossignol, Maura Ruzhnikov, Ralph Sacco, Jacinda B. Sampson, Mario Saporta, C. Ron Scott, Judy Schaechter, Timothy Schedl, Kelly Schoch, Daryl A. Scott, Vandana Shashi, Jimann Shin, Edwin K. Silverman, Janet S. Sinsheimer, Kathy Sisco, Edward C. Smith, Kevin S. Smith, Emily Solem, Lilianna Solnica-Krezel, Ben Solomon, Rebecca C. Spillmann, Joan M. Stoler, Jennifer A. Sullivan, Kathleen Sullivan, Angela Sun, Shirley Sutton, David A. Sweetser, Virginia Sybert, Holly K. Tabor, Amelia L.M. Tan, Queenie K.-G. Tan, Mustafa Tekin, Fred Telischi, Willa Thorson, Cynthia J. Tifft, Camilo Toro, Alyssa A. Tran, Brianna M. Tucker, Tiina K. Urv, Adeline Vanderver, Matt Velinder, Dave Viskochil, Tiphanie P. Vogel, Colleen E. Wahl, Stephanie Wallace, Nicole M. Walley, Melissa Walker, Jennifer Wambach, Jijun Wan, Lee-kai Wang, Michael F. Wangler, Patricia A. Ward, Daniel Wegner, Monika Weisz-Hubshman, Mark Wener, Tara Wenger, Katherine Wesseling Perry, Monte Westerfield, Matthew T. Wheeler, Jordan Whitlock, Lynne A. Wolfe, Kim Worley, Changrui Xiao, Shinya Yamamoto, John Yang, Diane B. Zastrow, Zhe Zhang, Chunli Zhao, Stephan Zuchner, Hugo Bellen, Rachel Mahoney.

Author Information

Conceptualization: S.P.S., K.A.R., K.L., K.G.; Data Curation: L.L., A.E., B.W., P.R.S., J.K., L.A., K.G.M.; Funding Acquisition: S.P.S., K.L., U.D.N, J.K., J.S., R.S., Investigation: S.P.S., K.A.R., K.L., K.G., F.S.A., J.K., K.G.M.; Methodology: S.P.S, L.L., B.W., J.K., L.A., J.H., K.M., K.Ü., M.A., P.R.S., R.S., F.S.A., U.B., L.A.E.; Project Administration: S.P.S., K.G., K.L., K.R.; Resources: S.P.S., K.L., U.D.N., R.S., U.B., L.A.E.; Software: P.R.S.; Supervision: S.P.S., K.L., K.G., L.A.E., R.S., F.S.A.; Visualization: S.P.S.; Writing-original draft: S.P.S. S.P.S., K.G., L.L., A.E., B.W., J.H., L.A., K.M., K.Ü., K.G.M., J.K., U.D.N., J.S., M.A., P.R.S., R.S., F.S.A., U.B., L.A.E., K.L., K.A.R. contributed to drafting the work, reviewed and approved the final submitted version, and agreed to be accountable for all aspects of the work.

Ethics Declaration

Study participants were recruited after obtaining appropriate Institutional Review Board review, approval, and consent at each institute, University of California, Davis, Sacramento; Boston Children's Hospital, Boston; and King Faisal Specialist Hospital and Research Center, Riyadh. Permission was received for use of photos and clinical information. In addition, the *Dph5*_p.His260Arg mouse model was developed and analyzed under an approved protocol reviewed by the University of California, Davis Institutional Animal Care and Use Committee and in accordance with the Association for Assessment and Accreditation of Laboratory Animal Care, International, and the Office of Laboratory Animal Welfare.

Conflicts of Interest

K.G.M. is an employee of GeneDx, Inc. K.M. and U.B. are members of and employed by Roche Pharma Research & Early Development. Roche is interested in targeted therapies and diagnostics.

Additional Information

The online version of this article (https://doi.org/10.1016/j.gim.2022.03.014) contains supplementary material, which is available to authorized users.

A novel *DPH5*-related diphthamide-deficiency syndrome causing embryonic lethality or profound neurodevelopmental disorder

Suma P. Shankar[1,2,*], **Kristin Grimsrud**[3,4], **Louise Lanoue**[4], **Alena Egense**[1], **Brandon Willis**[4], **Johanna Hörberg**[5], **Lama Albadi**[6,7], **Klaus Mayer**[8], **Koray Ütkür**[9], **Kristin G. Monaghan**[10], **Joel Krier**[11,12], **Joan Stoler**[12,13], **Maha Alnemer**[14], **Prabhu R. Shankar**[15], **Raffael Schaffrath**[9], **Fowzan S. Alkuraya**[7], **Ulrich Brinkmann**[8], **Leif A. Eriksson**[5], **Kent Lloyd**[4,16], **Katherine A. Rauen**[1] **Undiagnosed Diseases Network**[12]

[1]Division of Genomic Medicine, UC Davis MIND Institute, Department of Pediatrics, University of California, Davis, Sacramento, CA

[2]Department of Ophthalmology, University of California, Davis, Sacramento, CA

[3]Department of Pathology and Laboratory Medicine, University of California, Davis, Sacramento, CA

[4]UC Davis Mouse Biology Program, University of California, Davis, Davis, CA

[5]Department of Chemistry and Molecular Biology, University of Gothenburg, Gothenburg, Sweden

[6]Department of Zoology, College of Science, King Saud University, Riyadh, Saudi Arabia

[7]Department of Translational Genomics, Center for Genomic Medicine, King Faisal Specialist Hospital and Research Center, Riyadh, Saudi Arabia

[8]Roche Pharma Research and Early Development, Roche Innovation Center, Penzberg, Germany

[9]Division of Microbiology, Institute of Biology, University of Kassel, Kassel, Germany

[10]GeneDx, Gaithersburg, MD

[11]Division of Genetics, Brigham and Women's Hospital, Boston, MA

[12]Undiagnosed Diseases Network

[13]Division of Genetics and Genomics, Boston Children's Hospital, Boston, MA

[14]Department of Obstetrics & Gynecology, King Faisal Specialist Hospital and Research Center, Riyadh, Saudi Arabia

[15]Division of Health Informatics, Department of Public Health Sciences, University of California, Davis, Sacramento, CA

[16]Department of Surgery, University of California, Davis, Sacramento, CA

Abstract

Purpose: Diphthamide is a post-translationally modified histidine essential for messenger RNA translation and ribosomal protein synthesis. We present evidence for *DPH5* as a novel cause of embryonic lethality and profound neurodevelopmental delays (NDDs).

Methods: Molecular testing was performed using exome or genome sequencing. A transgenic *Dph5* knockin mouse (C57BL/6Ncrl-*Dph5*^{em1Mbp}/Mmucd) was created for a *DPH5* p.His260Arg homozygous variant identified in 1 family. Adenosine diphosphate–ribosylation assays in *DPH5*-knockout human and yeast cells and in silico modeling were performed for the identified *DPH5* potential pathogenic variants.

Results: *DPH5* variants p.His260Arg (homozygous), p.Asn110Ser and p.Arg207Ter (heterozygous), and p.Asn174LysfsTer10 (homozygous) were identified in 3 unrelated families with distinct overlapping craniofacial features, profound NDDs, multisystem abnormalities, and miscarriages. *Dph5* p.His260Arg homozygous knockin was embryonically lethal with only 1 subviable mouse exhibiting impaired growth, craniofacial dysmorphology, and multisystem dysfunction recapitulating the human phenotype. Adenosine diphosphate–ribosylation assays showed absent to decreased function in *DPH5*-knockout human and yeast cells. In silico modeling of the variants showed altered DPH5 structure and disruption of its interaction with eEF2.

Conclusion: We provide strong clinical, biochemical, and functional evidence for *DPH5* as a novel cause of embryonic lethality or profound NDDs with multisystem involvement and expand diphthamide-deficiency syndromes and ribosomopathies.

Keywords

Nonverbal neurodevelopment delays; Novel gene discovery; Precision animal modeling; Precision genomics; Translational genetics

Introduction

Neurodevelopmental disorders (NDDs) are genetically heterogeneous lifelong conditions that affect more than 3% of the pediatric population.[1] NDDs include global developmental delays; speech, language, and communication impairments; social and behavior issues; autism spectrum disorders; and neuropsychiatric conditions with high clinical variability; often, NDDs also have associated neurologic or multisystem involvement. Despite the increasing use of next generation sequencing methods, including exome sequencing (ES), genome sequencing (GS), and RNA sequencing, the underlying genetic etiology can be identified only in 9% to 50% of individuals with the highest yield among those with profound NDDs, including intellectual disabilities, epilepsy, and multisystem involvement.[1–6] We sought to determine the molecular basis of individuals with nonverbal NDDs in the Precision Genomics program, a novel initiative at University of California, Davis (UCD), Sacramento, to promote translational research. We used deep phenotyping and clinical ES and GS to obtain an accurate genetic diagnosis that can be returned to patients and their families. We collaborated with the UC Davis Mouse Biology Program to create targeted mouse models to determine the pathogenicity of variants of unknown significance (VUS) and/or genes of unknown significance to advance translational genomics and provide precision health care.

Through this program, we identified our index family harboring a rare homozygous missense variant p.His260Arg in *DPH5* (OMIM 611075) as a potential cause of profound NDDs in 2 affected siblings. Diphthamide is a post-translationally modified amino acid

histidine ineEF2 that is highly conserved from archaebacteria to humans.[7–10] eEF2 is essential for ribosomal translocation during messenger RNA (mRNA) translation and protein synthesis in cells.[11] The exact role of diphthamide is unclear; however, it serves as a target for bacterial adenosine diphosphate (ADP)-ribosylating toxins such as diphtheria toxin (DT) and Pseudomonas exotoxin A that inactivates eEF2 and stops protein synthesis in cells.[10,12] The biosynthesis of diphthamide is complex and involves multiple components, namely DPH1 to DPH7 along with the methylating cofactor S-adenosyl methionine (SAM).[13,14] To date, *DPH5* has not been reported as a disease-causing gene, although pathogenic variants in *DPH1* have been reported as causing autosomal recessive intellectual disability with distinct craniofacial features, CNS abnormalities, seizures, and digital abnormalities.[15–17] Given the similarities in the phenotype, *DPH5* was hypothesized as the potential causative gene in our subjects, and a targeted knockin mouse model for the p.His260Arg variant was initiated. While the mouse phenotyping was on-going, *DPH2* pathogenic variants were also reported as causing NDDs and craniofacial dysmorphology similar to *DPH1* disorder in 2 independent families by Hawer et al,[18] who proposed that *DPH1*- and *DPH2*-related disorders were diphthamide-deficiency syndromes and ribosomopathies. Furthermore, 2 additional unrelated families with rare variants in *DPH5* were identified through GeneMatcher.

In this study, we reported that biallelic, pathogenic homozygous, and compound heterozygous variants in *DPH5* cause profound NDDs with distinct craniofacial features and multisystem involvement in 3 unrelated families. We reported that homozygous predicted loss-of-function (LoF; frameshift) variant results in more severe disorder with miscarriages, still birth, and neonatal mortality. We presented evidence to prove pathogenicity of the *DPH5* variants using functional studies, biochemical tests, and computational modeling and proposed that *DPH5*-related diphthamide-deficiency syndrome is a novel autosomal recessive Mendelian disorder.

Materials and Methods

Human subjects

Study participants were recruited after obtaining Institutional Review Board approved consent at each institute, namely UCD; Boston Children's Hospital (BCH), Boston; and King Faisal Specialist Hospital and Research Center, Riyadh. Five affected individuals, their parents, and an unaffected sibling from 3 unrelated families participated in clinical and research genetic studies. Detailed phenotyping was performed in family 1 by S.P.S. at UCD, family 2 by J.S. at BCH, and family 3 by F.S.A. at King Faisal Specialist Hospital and Research Center. Children in Family 1 and 2 presented to the clinic with profound NDDs. In the neonate intensive care unit, family 3 was identified immediately after birth. The national and international collaboration was established through GeneMatcher.[19]

ES and GS

ES was performed for family 1 by GeneDx,[20] family 2 underwent clinical GS at Baylor through UDN,[21] and family 3 underwent ES in Saudi Arabia as previously described.[22]

Mouse knockin model

The *Dph5*_His260Arg mouse model was developed and analyzed under an approved protocol reviewed by the UCD Institutional Animal Care and Use Committee and in accordance with the Association for Assessment and Accreditation of Laboratory Animal Care, International, and the Office of Laboratory Animal Welfare. All mice were housed and cared for in accordance with the Guide for the Care and Use of Laboratory Animals Eighth Edition.[23] Mice were socially housed in individually ventilated cages (Optimice IVC, Animal Care Systems) on a 12:14 hour (6 AM to 8 PM) light cycle during the production phase and on a 12:12 hour (6 AM to 6 PM) light cycle during maintenance. Temperature ranges in the room were maintained between 68 and 79 °F, and mice were maintained on standard laboratory rodent chow (Rodent chow, Envigo 2918).

To study the in vivo functional impact of the p.His260Arg variant in *DPH5*, a targeted murine knockin of the homologous p.His260Arg was achieved using clustered regularly interspaced short palindromic repeats (CRISPR)/Cas9 genome editing (Supplemental Figure 1A). Briefly, single-cell C57BL/6N mouse zygotes were harvested from superovulated females and electroporated using standard protocols encompassing CRISPR ribonucleic protein and a single-stranded DNA oligonucleotide repair template to result in homology-directed repair of the desired region. The CRISPR ribonucleoprotein cleaves the mouse genome, and homology-directed repair of the knockin segment was assisted by the single-stranded DNA oligonucleotide repair template containing the desired change p.His260Arg (Supplemental Figure 1A–E, Supplemental Table 1).

The genetically manipulated embryos were surgically transferred into the oviducts of pseudopregnant CD1 female mice, and after gestation, pre-weaned mouse pups were sampled and genetically tested by end point polymerase chain reaction (PCR) and sequencing to definitively identify founder mice harboring the desired pathogenic variant, p.His260Arg. Two founder mice were successfully generated and bred with C57BL/6N wild-type (WT) mice for generation of germline transmission mice (N1). The N1 mice genotypes were confirmed by PCR, and heterozygous animals were intercrossed to generate the desired cohorts of male and female homozygous mice for phenotyping analysis.

Embryo collection and micro computed tomography imaging

Embryos were dissected from pregnant females on embryonic day 18.5 and transferred to heparinized (1 U/mL phosphate-buffered saline [PBS]) Ca^{2+}/Mg^{2+}free PBS at 37 °C. The placenta and umbilical cord were sectioned, and the yolk sacs were collected for genotyping. The embryos were euthanized by exsanguination and submerged in 4% paraformaldehyde (PBS) fixative for 4 to 5 days at 4 °C on a rocker and stored at 4 °C in PBS containing 0.02% sodium azide until processed for micro computed tomography (μCT). Please see Supplemental Data for additional methods and imaging details.

Phenotyping assessment tests

The heterozygous mice underwent extensive phenotyping from age 5 weeks, including weekly body weight measurements, SHIRPA, grip strength, open field, marble burying, social and object novelty, acoustic startle, X-rays, auditory brain response, and gross

pathology at necropsy. The schedule of the phenotyping assays and detailed descriptions of the phenotyping tests are included in the Supplemental Data.

In silico modeling

Homology models of WT and p.His260Arg, p.Asn110Ser, p.Arg207Ter, and p.Asn174LysfsTer10 variants of human *DPH5* were generated with the program Yet Another Scientific Artificial Reality Application,[24,25] using the DPH5 crystal structures of *Entamoeba histolytica* (PDB-ID 3I4T) and *Pyrococcus hirokoshii* (PDB-ID 2EGL, 2DXW, 2Z6R and 2E7R) as templates. All homology modeling (HM) was conducted using the default settings in the macro hm_build.mcr and involved BLAST-searches, multiple sequence alignments, loop modeling and refinement, and molecular dynamics based simulated annealing minimization. The quality of each model was assessed during the HM computations using *z*-scores based on dihedrals and 1-dimensional and 3-dimensional packing. For each system, between 5 and 8 initial HM models were generated followed by construction of the best hybrid model. For a better understanding of the effect of different pathogenic variants, the hybrid models were then superposed onto our previous model of the DPH5-eEF2 complex of *Saccharomyces cervisae*[6] and the *S cervisae* DPH5 model deleted (retaining SAM and eEF2). All structural analyses were conducted using Molecular Operating Environment 2018.0101[26].

Analyses of *DPH5* variants in recombinant MCF7 *DPH5*-K0 complementation assays

MCF7 breast cancer cell line–derived *DPH5*-knockouts (KOs) were used as described previously to assess the effect of *DPH5*, p.Asn110Ser, p.Asn174LysfsTer10, p.Arg207Ter, and p.His260Arg variants on diphthamide synthesis.[27] Radioimmunoprecipitation assay buffer extracts of the *DPH5*-KO cells that were transfected with recombinant expression plasmids encoding *DPH5* WT and p.Asn110Ser, p.Asn174LysfsTer10, p.Arg207Ter, and p.His260Arg variants were exposed to DT and biotinylated nicotinamide adenine dinucleotide (Bio-NAD) for an hour at 25 °C. The extracts were then subjected to reducing sodium dodecyl sulfate–polyacrylamide gel electrophoresis and blotted to membranes that were probed with streptavidin–horseradish peroxidase and peroxidase substrate to detect the presence of biotinylated eEF2. The presence of diphthamide (generated by recombinant *DPH5* in the *DPH5*-KO background) results in a band at approximately 100kDa. Additional details of ADP-ribosylation assays are similar to that described previously by Mayer et al.[28] It is important to note that such assays provide variant proteins via recombinant multicopy expression. Therefore, enzymes with reduced activities can still help in the synthesis of diphthamide if increased expression levels compensate their partial inactivation.

Yeast cultivation and mutagenesis

To overcome limitations of MCF7 assays caused by multicopy expression of variant *DPH5*, ADP-ribosylation and phenotype assays of *S cerevisiae* variants harboring single-copy chromosome–encoded *DPH5* variants can be applied. DPH5 enzymes are highly conserved among eukaryotes, including yeast, and human pathogenic variants, namely p.Asn110, p.Asn174, p.Arg206, and p.His260, corresponding to the *S cerevisiae* variants p.Asn111, p.Asn175, p.Arg205, and p.His257 were identified (Supplemental Figure 3). Yeast strains used and generated for this study are listed in Supplemental Table 3. Genomic

dph5 missense variants p.Asn111Ser (human p.Asn110Ser) and p.His257Arg (human p.His260Arg) were generated using the 2-step method for the introduction of missense variants as described previously.[29] PCR-mediated pUG27 cassettes[30] were integrated into the 3′-untranslated region of *dph5* in BY4741 cells using standard lithium acetate transformation and selection on minimal yeast nitrogen base (YNB) medium lacking histidine. Correct insertion of the pUG27 cassette was verified by diagnostic PCR with primers positioned outside the *dph5* locus (Supplemental Table 4). Site-directed mutagenesis PCR was performed on a fragment consisting of *dph5*, including the pUG27 cassette in the 3′-untranslated region inserted in a pJET1.2 cloning vector (Thermo Fisher scientific; catalog number 1231). The resulting potential pathogenic variants were amplified via PCR and transformed in cells via pUG73-based *dph5* disruption. After recovery on yeast extract peptone dextrose plates at 30 °C overnight, counterselection was performed by growing cells in liquid YNB media lacking histidine and containing 1 g/L 5′-fluorootic acid at 30 °C for 8 hours and plating 50 μL of the liquid culture on YNB-plates lacking histidine and containing 5′-fluorootic acid (1 g/L). Resulting variant cells were verified using standard colony PCR protocols and DNA sequencing of PCR products amplified from genomic DNA.

Yeast ADP-ribosylation assays

ADP-ribosylation assays were performed with total protein extracts of the yeast BY4741 strains for WT, *dph5*-KO, and the 2 missense variants, p.Asn111Ser and p.His257Arg, whose activities could not be differentiated from WT DPH5 in MCF7 assays. The presence or absence diphthamide was assessed by incubating the extracts with DT and biotinylated nicotinamide adenine dinucleotide. The presence of diphthamide results in successful ADP-ribosylation and generates biotinylated eEF2. This can be detected by sodium dodecyl sulfate–polyacrylamide gel electrophoresis blots probed with streptavidin–horseradish peroxidase and peroxidase substrate.[28]

Yeast phenotypic assays

Phenotypic assays of WT *dph5* and variant *dph5* yeast derivatives were performed by spotting 10-fold cell dilutions starting at optical density (600 nm) of 1 on full yeast extract peptone dextrose media containing 80 or 100 μg/μL hygromycin B. A plasmid carrying the catalytic ADP-ribosylation domain of DT fused to a galactose-inducible promoter (pSU8)[31] was transformed into WT *dph5* and potential pathogenic variants to assess intracellular activity of the toxin. For the DT assay, cells were spotted in 10-fold serial cell dilutions starting at optical density (600 nm) of 1 on YNB medium lacking leucine and containing the indicated concentrations of raffinose and galactose. All plates were incubated for 2 to 3 days at 30 °C.

Results

Patient studies

We report on 5 individuals, 3 females and 2 males from 3 unrelated families with variants in *DPH5*, ages ranging from 11 days to 10 years. Family 1 is a consanguineous Syrian family with 2 siblings presenting with profound NDDs and intellectual disability, remaining nonverbal with an inability to function independently. The older 10-year-old female carried a

diagnosis of congenital hypotonia and cerebral palsy. She was born at 42 weeks gestational age with a history of intrauterine growth retardation and macrocephaly at birth per parental report (currently she is normocephalic). She presented with dysphagia and failure to thrive and required gastrostomy-jejunostomy tube feeds. She was crawling for ambulation until age 9 years, after which she has been able to walk a few steps independently, albeit with an unsteady gait. She had distinct craniofacial features, including broad forehead, sparse eyebrows, epicanthal folds, short nose with upturned tip, downturned corners of the mouth, poor dentition, tapering fingers, and short third toes, bilaterally (Figure 1A). Her younger sibling, an 8-year-old male, also presented with profound NDDs and intellectual disability, remaining nonverbal; he was crawling but not walking, had infantile onset seizures, and was dysphagic and required gastrostomy-jejunostomy tube feeds. He had facial features similar to his sister and, in addition, had ocular melanocytosis, pathologic high myopia, and brachydactyly (Figure 1B and 1G). Additional clinical features and investigations are summarized in Table 1 as family 1, individuals A and B. Family history was significant for consanguinity and a male sibling who died at age 1 week in a hospital in Syria (Figure 1J, family 1). ES (Materials and Methods) revealed a homozygous variant of uncertain significance (VUS) in *DPH5*, NM_001077394.2:c.779A>G, p.His260Arg (NC_000001.11:g.100990487T>C; Genome Aggregation Database [gnomAD] v3.1.1, minor allele frequency [MAF] = 6.57×10^{-6})[32] in the 2 affected siblings with an unaffected sister and both parents being heterozygous for the *DPH5* variant.

Family 2 was recruited from BCH and had 2 affected siblings harboring *DPH5* compound heterozygous variants in *trans*: (1) NM_001077394.2:c.619C>T, p.Arg207Ter (NC_000001.11:g.100992652G>A; MAF = 2.631×10^{-5})[32] and (2) NM_001077394.2:c.329A>G, p.Asn110Ser (NC_000001.11:g.101013750T>C; MAF = 1.204×10^{-5}).[32] The older sibling, a 9-year-old male, presented with profound NDDs and intellectual disability, remained nonverbal, and had a history of seizures and congenital aortic dilatation. He had distinct facial features, including broad forehead, depressed midface, upslanting palpebral fissures, sparse eyelashes, mild epicanthal folds, thick alveolar ridges, and gray sclera with ocular melanocytosis similar to affected individuals in family 1 (Figure 1C, Table 1, family 2, individual A). His 1-year-old sister also had profound NDDs, seizures, and congenital aortic dilatation with facial features similar to her brother (Figure 1D, Table 1, family 2, individual B). Parents were of European ancestry and nonconsanguineous with 4 other siblings unaffected (Figure 1J, family 2).

Family 3 harbored a *DPH5* homozygous VUS, NM_001077394.2:c.521dup (p.Asn174LysfsTer10) variant (NC_000001.11:g.100995122dup; absent in gnomAD)[32] in a preterm female. She had ventricular septal defect, pulmonary stenosis, pericardial effusion, brachycephaly, and an enlarged cistema magna. Her facial features included broad forehead, bitemporal narrowing, sparse eyebrows, epicanthal folds, wide palpebral fissures, broad nasal bridge, rounded nasal tip, downturned corners of mouth, and triangular chin, which were similar to individuals in families 1 and 2 (Figure 1E). She died at age 11 days owing to multisystem complications. Chest and abdominal X-ray showed evidence of extensive pneumoperitoneum due to bowel perforation (Figure 1F). Brain magnetic resonance imaging showed bilateral minimal tentorial subdural hemorrhages and enlarged cisterna magna with normal myelination and gyration (Figure 1G, Table 1, family 3A). Family history was

significant for consanguinity and multiple spontaneous miscarriages, 1 stillbirth, and 1 neonatal death (Figure 1J, family 3).

Murine modeling

The orthologous *Dph5*_p.His260Arg targeted murine knockin were generated using C57BL/6N embryonic stem cells and backcrossed to C57BL/6N mice. A total of 43 pups were born from a series of intercross breeding producing 7 litters (14 WT, 28 heterozygous, and 1 homozygous). The 1 subviable live homozygous female mouse exhibited extreme low birthweight, rounded head and short blunted snout, polydactyly on 1 foot, a depigmented patch on the abdomen, and abnormal behavior with obsessive grooming of the face when held (Figure 2A–C). The female mouse was found dead at age 24 days, and necropsy showed autolyzed tissues and hemorrhage around the lambdoid sutures of the skull (Figure 2D).

The additional breeding of *Dph5*_p.His260Arg heterozygous mice to further evaluate the subviability of homozygous mice resulted in gravid heterozygous females. In total, 20 embryos from 3 heterozygous females were harvested on embryonic day 18.5 days for gross morphology and μCT evaluation. Yolk sac genotyping of 14 male and 6 female embryos identified 7 WT, 6 heterozygous, and 7 homozygous embryos. All WT and heterozygous *Dph5*_p.His260Arg embryos were of typical development. All 7 homozygous embryos were small, and gross morphological examination revealed a fully penetrant phenotype as all 7 embryos presented with a range of anomalies with varying degree of severity, including polydactyly (4/7), eye anomalies (4/7), edema (3/7), shortened frontonasal prominence (2/7), facial cleft (2/7), abnormal head shape (2/7), and exencephaly (1/7) (Figure 2E). The μCT images revealed a range of findings, including facial clefts, microphthalmia, anophthalmia, exencephaly, shortened frontonasal prominence, vascular hemorrhages with edema, situs inversus of the dorsal aorta, and ventricular septal defects recapitulating the human phenotype (Figures 2F–2J, Supplemental Table 2). The viable WT and all but 2 of the 28 heterozygous mice were of typical development. The 2 atypical heterozygous *Dph5*_p.Hi-s260Arg mice exhibited craniofacial dysmorphology, decreased body weight, and reduced neuromuscular function. However, when the mice were euthanized at 16 weeks, no major organ abnormalities were identified by necropsy and histology (Supplemental Figure 2). While these findings in the 2 atypical heterozygote mice are not consistent with that in heterozygote humans who have no craniofacial dysmorphic features or other clinical manifestations, some differences in phenotype between mice and humans are expected. Depending on the genetic background of the inbred mice, when human knockin variants are tested in mice, there is a high likelihood that the phenotype observed may be more (or less) intense than in the human patient. We created these pathogenic variants on an inbred background, which increases the possibility of any potential genetic modifiers to be homozygous compared with that in the humans who are outbred and less likely to be homozygous at any modifier loci. For the *Dph5* p.His260Arg variant, given that we observed a very severe phenotype (late embryonic/postnatal death) in the homozygous mouse than in the homozygous human, it is plausible to see milder observable phenotypes in the heterozygous mouse that may partially mimic the phenotype(s) seen in the patient, even though it is a recessive disorder in humans.

In silico modeling

The in silico models created using Yet Another Scientific Artificial Reality Application and Molecular Operating Environment 2018.0101 for DPH5 p.His260Arg showed protein structure and folding similar to WT; however, it resulted in a positive charge with repulsion and weakening of the DPH5 interaction with eEF2 (Figure 3A–3D). DPH5 p.Asn110Ser seemed to weaken dimer stability impairing DPH5-eEF2 interaction (Figure 3E). The premature stop

p.Arg207Ter and p.Asn174LysfsTer10 variants occur in the terminal exon of *DPH5* and are not expected to be subject to nonsense mediated decay. The DPH5 p.Arg207Ter truncating variant removed a significant portion of DPH5 and disrupted interaction with eEF2 (Figure F and G). The DPH5 p.Asn174LysfsTer10 truncates the DPH5 protein surface causing significantly reduced interaction with eEF2 and a solvent exposed SAM (Figure H and I).

Analyses of *DPH5* variants in recombinant MCF7-DPH5ko complementation assays

DT exclusively ADP-ribosylates eEF2 that harbors diphthamide. ADP-ribosylation assays based on recombinant expression of variant DPH5 enzymes in DPH5 deficient human MCF7 cells can hence be applied for sensitive detection of diphthamide synthesis. The absence of ADP-ribosylation signals in turn reflects the loss of functionality of variant DPH5 enzymes.[14,28] The results of ADP-ribosylation analyses of DPH5 enzymes carrying the human variants reveal total lack of enzymatic activity for p.Arg207Ter (c.619C>T) and minimal signal detectable for p.Asn174Lysfs (c.521dupA) (Figure4A). However, p.Asn110Ser (c.329A>G) and p.His260Arg (c.779A>G) revealed residual activities sufficient to provide diphthamide-eEF2 upon multicopy plasmid-driven expression in MCF7-DPH5ko as shown by robust detection of biotinylated eEF2 (Figure 4A).

Analyses of *DPH5* variants in *S cerevisiae*

The MCF7 assay is consistent with DPH5-deficient phenotypes for individuals who carry homozygous p.Asn174LysfsTer10 alleles. Individuals with homozygous p.His260Arg or compound heterozygous p.Arg207Ter and Asn110Ser alleles, however, cannot be unambiguously called DPH5-compromised based on MCF7-DPHko results. MCF7 assays provide variant proteins via recombinant multicopy expression. Enzymes with reduced activities may still help in the synthesis of diphthamide if increased expression levels compensate for their partial inactivation. This assay limitation can be overcome with *S cerevisiae* variants harboring single-copy chromosome–encoded *DPH5* variants at those positions that were identified in patients. Given DPH5 enzymes are highly conserved among eukaryotes, including yeast, p.Asn110, p.Asn174, p.Arg206, and p.His260 in human *DPH5* corresponding to p.Asn111, p.Asn175, p.Arg205, and p.His257 were identified in *S cerevisiae* (Supplemental Figure 3). The *S cerevisiae* system not only provides *DPH5* variants in single-copy chromosome–encoded form for in vitro

ADP-ribosylation assays, but also enables the assessment of phenotypes: yeast cells with reduced or no diphthamide show resistance to ADP-ribosylating DT and hypersensitivity toward the aminoglycoside antibiotic hygromycin.[18] The analyses of the *DPH5* variants p.Asn110Ser and p.His260Arg (yeast equivalents p.Asn111Ser and p.His257Arg) revealed

the presence of diphthamidylated eEF2 in both strains. Thus, both variants retain sufficient activity to still produce diphthamide in yeast that generate signals indistinguishable from WT by toxin-induced ADP-ribosylation (Figure 4B). In contrast, the (more sensitive) phenotype assays indicated that diphthamide synthesis was partially compromised, resulting in intermediate phenotypes (Figure 4C and 4D). Both missense variant strains tolerated DT better than WT cells but were not as resistant as strains with completely inactivated DPH5 (Figure 4C). In addition, both variant strains were more sensitive to hygromycin than WT cells but less sensitive than strains with completely inactivated DPH5 (Figure 4D).

Discussion

We identified biallelic variants in *DPH5*, including homozygous p.His260Arg, compound heterozygous p.Arg207Ter in *trans* with p.Asn110Ser, and homozygous p.Asn174LysfsTer10 in 3 unrelated families and described their phenotype characterized by distinct craniofacial features, multisystem dysfunction, profound NDDs, multiple miscarriages, and neonatal death (Table 1). Individuals of all 3 families shared craniofacial features, which included broad forehead, frontal bossing, sparse hair and eyebrows, epicanthal folds, broad nasal bridge with rounded nasal tip, and triangular chin; all were normocephalic and had short stature and failure to thrive before G tube placement. Two families had a history of miscarriages and early infant deaths. All had profound NDDs, with intellectual disability remaining nonverbal with poor mobility and inability to function independently. Cardiac features and respiratory system involvement were variable. All had hypotonia or peripheral spasticity with brain magnetic resonance imaging findings ranging from normal to diffuse paucity of white matter to cerebellar atrophy. We also noted similar cranioectodermal features and multisystem involvement with autosomal recessive mode of inheritance for *DPH1* and *DPH2*,[18,33] disorders, whereas de novo variants in *EEF2* cause similar craniofacial features but milder NDDs[34] (Supplemental Table 5). In addition, a missense variant in *EEF2* was reported as causing autosomal dominant spinocerebellar ataxia type 25 affecting multiple generations in 1 family but with no other NDDs.[34]

In this study, we provided in vivo and in vitro functional studies and computational modeling data to prove pathogenicity of the *DPH5* variants and propose *DPH5* as a novel cause of diphthamide-deficiency disorders. The human phenotype was recapitulated in the *Dph5*_pH260R knockin mouse model with multisystem abnormalities, including craniofacial, ophthalmologic, cardiac, visceral, and hemopoietic in most homozygous embryos that were nonviable. The only live born homozygous mouse exhibited extremely low birthweight, failure to thrive, craniofacial dysmorphology, polydactyly, unusual grooming behavior, and early death.

The in silico modeling with the observed variants revealed alterations of DPH5 protein structure or electrostatic charge differences that disrupted the interaction between DPH5 and eEF2 with implications on mRNA translation and protein synthesis. The ADP-ribosylation assays in MCF7 *DPH5*-KO cells revealed absent or decreased activity for DPH5 p.Arg207Ter, the premature stop variant, and the DPH5 p.Asn174LysfsTer10 frameshift variant that is predicted to result in aberrant charge and premature stop protein. Furthermore, phenotype analyses of yeast strains carrying missense variants corresponding to *DPH5*

p.Asn110Ser and *DPH5* p.His260Arg revealed reduced function of these variants evidenced by decreased DT and increased hygromycin-sensitivity.

DPH5 (OMIM 611075) is a methyl transferase with a highly conserved domain (Figure 1I) critical to the biosynthesis of diphthamide, a post-translationally modified amino acid histidine on eEF2 essential for ADP-ribosylation, mRNA translation, and protein synthesis.[13,14,18,35–37] A recent transcriptome study of *Dph5*-KO cells in the gut of adult *Drosophila* suggests that DPH5 has a role in the regulation of ribosome biogenesis genes.[38] DPH5 is ubiquitously expressed in all tissues in humans.[39] The complete absence of DPH5 function is not compatible with life as shown by the embryonic lethality of the *Dph5*$^{ko/ko}$ line (unpublished KOMP/Sanger data). Biallelic total or near total LoF pathogenic variants in humans may also result in abortions and early fetal losses as seen in family 3 harboring the homozygous frameshift variant p.Asn174FysfsTer10. Multiple miscarriages, still birth, and neonatal mortality were reported in this family. We postulated that the presence of residual DPH5 function results in live births with multisystem abnormalities and profound NDDs as seen in family 1 with the homozygous p.His260Arg missense variant and in family 2 with the compound heterozygous variants, p.Arg207Ter in *trans* with p.Asn110Ser. *DPH5* has a probability of being (LoF) intolerant score of 0 and an FoF observed/expected upper bound fraction of 0.77 (0.48-1.27) (gnomADv2.1.1),[32] suggesting the tolerance of *DPH5* to LoF in heterozygous state but not in homozygous state with compound heterozygotes probably retaining intermediate functionality.[32]

In summary, we provide clinical, molecular, functional, biochemical, and computational data as proof of pathogenicity for the *DPH5* variants p.Asn110Ser, p.Asn174LysfsTer10, p.Arg207Ter, and p.His260Arg, establishing *DPH5* related diphthamide-deficiency syndrome as a novel autosomal recessive disorder expanding the disorders caused by diphthamide biosynthesis pathway genes.[15,18,33]

Ribosome biogenesis is essential for mRNA translation, protein synthesis, and cell growth and proliferation. Defects in ribosome biogenesis have been reported to cause Treacher Collins Syndrome, Diamond-Blackfan anemia, and Shwachman-Diamond syndrome that are referred to as ribosomopathies.[40] However, in other putative ribosomopathies such as Blooms and Werner syndrome and cohesinopathies, the stress responses associated with ribosomal defects and/or mRNA translation alterations may contribute to disease phenotype and severity.[40] Diphthamide is essential for translational accuracy and ribosomal protein synthesis,[12,18] although additional studies are needed to understand the exact pathophysiology of diphthamide-deficiency disorders.

Our study highlights the power of clinical translational genomics and precision modeling in determining the pathogenicity of a VUS and accelerating new gene discoveries. Furthermore, the *Dph5* p.His260Arg mouse model serves as a valuable resource for understanding the critical role of diphthamide biosynthesis genes in organogenesis and development. In addition, it serves as a model for in vivo therapeutic options and advances in precision medicine.

Supplementary Material

Refer to Web version on PubMed Central for supplementary material.

Acknowledgments

S.P.S. is the Children's Miracle Network Endowed Chair in Pediatric Genetics and receives salary and grant support. Grant #U42 OD012210 (PI: K.L.; CI: S.P.S.) MMRRC Supplement and C57BL/6NCrl-*Dph5*$^{em1(IMPC)Mbp}$/Mmucd in MMRRC Repository. SCHA750/21-1 Support was provided by DFG Priority Program 1927 'Iron-Sulfur for Life' to R.S. National Institutes of Health (NIH) 1U41HG006834-01A1 grant support to U.D.N. was received by J.K. and J.S. NIH U01HG007690 was provided to Undiagnosed Diseases Network. We thank all patient families and the staff at the Mouse Biology Program for their contributions in developing and phenotyping this mouse model.

U.D.N. funding acknowledgment

Research reported in this manuscript was supported by the NIH Common Fund, through the Office of Strategic Coordination/Office of the NIH Director under Award Number U01HG007690. The content is solely the responsibility of the authors and does not necessarily represent the official views of the NIH.

Data Availability

We have presented data supporting the conclusions of this study within the main article and Supplemental Information. The authors are willing to share de-identified data sets, materials, methods, protocols, and procedures used in obtaining the results presented in this publication with other researchers on request.

References

1. Gilissen C, Hehir-Kwa JY, Thung DT, et al. Genome sequencing identifies major causes of severe intellectual disability. Nature. 2014;511(7509):344–347. 10.1038/nature13394. [PubMed: 24896178]
2. Ismail FY, Shapiro BK. What are neurodevelopmental disorders? Curr Opin Neurol. 2019;32(4):611–616. 10.1097/WCO.0000000000000710. [PubMed: 31116115]
3. Lee H, Nelson SF. The frontiers of sequencing in undiagnosed neurodevelopmental diseases. Curr Opin Genet Dev. 2020;65:76–83. 10.1016/j.gde.2020.05.003. [PubMed: 32599523]
4. Vissers LE, Gilissen C, Veltman JA. Genetic studies in intellectual disability and related disorders. Nat Rev Genet. 2016;17(1):9–18. 10.1038/nrg3999. [PubMed: 26503795]
5. Soden SE, Saunders CJ, Willig LK, et al. Effectiveness of exome and genome sequencing guided by acuity of illness for diagnosis of neurodevelopmental disorders. Sci Transl Med. 2014;6(265):265ra168. 10.1126/scitranslmed.3010076.
6. Guo H, Duyzend MH, Coe BP, et al. Genome sequencing identifies multiple deleterious variants in autism patients with more severe phenotypes. Genet Med. 2019;21(7):1611–1620. 10.1038/s41436-018-0380-2. [PubMed: 30504930]
7. Van Ness BG, Howard JB, Bodley JW. ADP-ribosylation of elongation factor 2 by diphtheria toxin. Isolation and properties of the novel ribosyl-amino acid and its hydrolysis products. J Biol Chem. 1980;255(22):10717–10720. [PubMed: 7000782]
8. Pappenheimer AM Jr, Dunlop PC, Adolph KW, Bodley JW. Occurrence of diphthamide in archaebacteria. J Bacteriol. 1983;153(3):1342–1347. 10.1128/jb.153.3.1342-1347.1983. [PubMed: 6402493]
9. Dunlop PC, Bodley JW. Biosynthetic labeling of diphthamide in Saccharomyces cerevisiae. J Biol Chem. 1983;258(8):4754–4758. [PubMed: 6339504]
10. Kaneda Y, Yoshida MC, Kohno K, Uchida T, Okada Y. Chromosomal assignment of the gene for human elongation factor 2. Proc Natl Acad Sci U S A. 1984;81(10):3158–3162. 10.1073/pnas.81.10.3158. [PubMed: 6427766]

11. Ueda K, Hayaishi O. ADP-ribosylation. Anna Rev Biochem. 1985;54:73–100. 10.1146/annurev.bi.54.070185.000445. [PubMed: 3927821]
12. Su X, Lin Z, Lin H. The biosynthesis and biological function of diphthamide. Crit Rev Biochem Mol Biol. 2013;48(6):515–521. 10.3109/10409238.2013.831023. [PubMed: 23971743]
13. Carette JE, Guimaraes CP, Varadarajan M, et al. Haploid genetic screens in human cells identify host factors used by pathogens. Science. 2009;326(5957):1231–1235. 10.1126/science.1178955. [PubMed: 19965467]
14. Schaffrath R, Abdel-Fattah W, Klassen R, Stark MJ. The diphthamide modification pathway from Saccharomyces cerevisiae–revisited. Mol Microbiol. 2014;94(6):1213–1226. 10.1111/mmi.12845. [PubMed: 25352115]
15. Alazami AM, Patel N, Shamseldin HE, et al. Accelerating novel candidate gene discovery in neurogenetic disorders via whole-exome sequencing of prescreened multiplex consanguineous families. Cell Rep. 2015;10(2):148–161. 10.1016/j.celrep.2014.12.015. [PubMed: 25558065]
16. Loucks CM, Parboosingh JS, Shaheen R, et al. Matching two independent cohorts validates DPH1 as a gene responsible for autosomal recessive intellectual disability with short stature, craniofacial, and ectodermal anomalies. Hum Mutat. 2015;36(10):1015–1019. 10.1002/humu.22843. [PubMed: 26220823]
17. Sekiguchi F, Nasiri J, Sedghi M, et al. A novel homozygous DPH1 mutation causes intellectual disability and unique craniofacial features. J Hum Genet. 2018;63(4):487–491. 10.1038/s10038-017-0404-9. [PubMed: 29410513]
18. Hawer H, Mendelsohn BA, Mayer K, et al. Diphthamide-deficiency syndrome: a novel human developmental disorder and ribosomopathy. Eur J Hum Genet. 2020;28(11):1497–1508. 10.1038/s41431-020-0668-y. [PubMed: 32576952]
19. Sobreira N, Schiettecatte F, Valle D, Hamosh A. GeneMatcher: a matching tool for connecting investigators with an interest in the same gene. Hum Mutat. 2015;36(10):928–930. 10.1002/humu.22844. [PubMed: 26220891]
20. Guillen Sacoto MJ, Tchasovnikarova IA, Torti E, et al. De novo variants in the ATPase module of MORC2 cause a neurodevelopmental disorder with growth retardation and variable craniofacial dysmorphism. Am J Hum Genet. 2020;107(2):352–363. 10.1016/j.ajhg.2020.06.013. [PubMed: 32693025]
21. Haghighi A, Krier JB, Toth-Petroczy A, et al. An integrated clinical program and crowdsourcing strategy for genomic sequencing and Mendelian disease gene discovery. NPJ Genom Med. 2018;3:21. 10.1038/s41525-018-0060-9. [PubMed: 30131872]
22. Monies D, Abouelhoda M, AlSayed M, et al. The landscape of genetic diseases in Saudi Arabia based on the first 1000 diagnostic panels and exomes. Hum Genet. 2017;136(8):921–939. 10.1007/s00439-017-1821-8. [PubMed: 28600779]
23. National Research Council (US) Committee. Guide for the Care and Use of Laboratory Animals. 8th ed. National Academies Press (US); 2011.
24. Hörberg J, Saenz-Mendez P, Eriksson LA. QM/MM studies of Dph5 - a promiscuous methyltransferase in the eukaryotic biosynthetic pathway of diphthamide. J Chem Inf Model. 2018;58(7):1406–1414. 10.1021/acs.jcim.8b00217. [PubMed: 29927239]
25. Krieger E, Vriend G. YASARA view - molecular graphics for all devices - from smartphones to workstations. Bioinformatics. 2014;30:2981–2982. 10.1093/bioinformatics/btu426. [PubMed: 24996895]
26. Chemical Computing Group ULC, M. Molecular operating environment (MOE) 2018.01. Canadian. http://www.chemcomp.com.
27. Stahl S, da Silva Mateus Seidl AR, Ducret A, et al. Loss of diphthamide pre-activates NF-κB and death receptor pathways and renders MCF7 cells hypersensitive to tumor necrosis factor. Proc Natl Acad Sci U S A. 2015;112(34):10732–10737. 10.1073/pnas.1512863112. [PubMed: 26261303]
28. Mayer K, Schröder A, Schnitger J, Stahl S, Brinkmann U. Influence of DPH1 and DPH5 protein variants on the synthesis of diphthamide, the target of ADPRibosylating toxins. Toxins (Basel). 2017;9(3):78. 10.3390/toxins9030078.

29. Toulmay A, Schneiter R. A two-step method for the introduction of single or multiple defined point mutations into the genome of Saccharomyces cerevisiae. Yeast. 2006;23(11):825–831. 10.1002/yea.1397. [PubMed: 16921548]
30. Gueldener U, Heinisch J, Koehler GJ, Voss D, Hegemann JH. A second set of loxP marker cassettes for Cre-mediated multiple gene knockouts in budding yeast. Nucleic Acids Res. 2002;30(6):e23. 10.1093/nar/30.6.e23. [PubMed: 11884642]
31. Uthman S, Bär C, Scheidt V, et al. The amidation step of diphthamide biosynthesis in yeast requires DPH6, a gene identified through mining the DPH1-DPH5 interaction network. PLoS Genet. 2013;9(2):e1003334. 10.1371/journal.pgen.1003334. [PubMed: 23468660]
32. Karczewski KJ, Francioli LC, Tiao G, et al. The mutational constraint spectrum quantified from variation in 141,456 humans. Nature. 2020;581(7809):434–443. Published correction appears in *Nature*. 2021;590(7846):E53. Published correction appears in *Nature*. 2021;597(7874):E3-E4. 10.1038/s41586-020-2308-7. [PubMed: 32461654]
33. Urreizti R, Mayer K, Evrony GD, et al. DPH1 syndrome: two novel variants and structural and functional analyses of seven missense variants identified in syndromic patients. Eur J Hum Genet. 2020;28(1):64–75. 10.1038/s41431-019-0374-9. Published correction appears in *Eur J Hum Genet.* 2020;28(1):138. [PubMed: 30877278]
34. Nabais Sá MJ, Olson AN, Yoon G, et al. De novo variants in EEF2 cause a neurodevelopmental disorder with benign external hydrocephalus. Hum Mol Genet. 2021;29(24):3892–3899. 10.1093/hmg/ddaa270. [PubMed: 33355653]
35. Hawer H, Ütkür K, Arend M, et al. Importance of diphthamide modified EF2 for translational accuracy and competitive cell growth in yeast. PLoS One. 2018;13(10):e0205870. 10.1371/journal.pone.0205870. [PubMed: 30335802]
36. Mattheakis LC, Shen WH, Collier RJ. DPH5, a methyltransferase gene required for diphthamide biosynthesis in Saccharomyces cerevisiae. Mol Cell Biol. 1992;12(9):4026–4037. 10.1128/mcb.12.9.4026-4037.1992. [PubMed: 1508200]
37. Liu S, Milne GT, Kuremsky JG, Fink GR, Leppla SH. Identification of the proteins required for biosynthesis of diphthamide, the target of bacterial ADP-ribosylating toxins on translation elongation factor 2. Mol Cell Biol. 2004;24(21):9487–9497. 10.1128/MCB.24.21.9487-9497.2004. [PubMed: 15485916]
38. Tsuda-Sakurai K, Kimura M, Miura M. Diphthamide modification of eEF2 is required for gut tumor-like hyperplasia induced by oncogenic Ras. Genes Cells. 2020;25(2):76–85. 10.1111/gtc.12742. [PubMed: 31828897]
39. Thul PJ, Åkesson L, Wiking M, et al. A subcellular map of the human proteome. Science. 2017;356(6340). 10.1126/science.aal3321.
40. Kang J, Brajanovski N, Chan KT, Xuan J, Pearson RB, Sanij E. Ribosomal proteins and human diseases: molecular mechanisms and targeted therapy. Signal Transduct Target Ther. 2021;6(1):323. 10.1038/s41392-021-00728-8. [PubMed: 34462428]

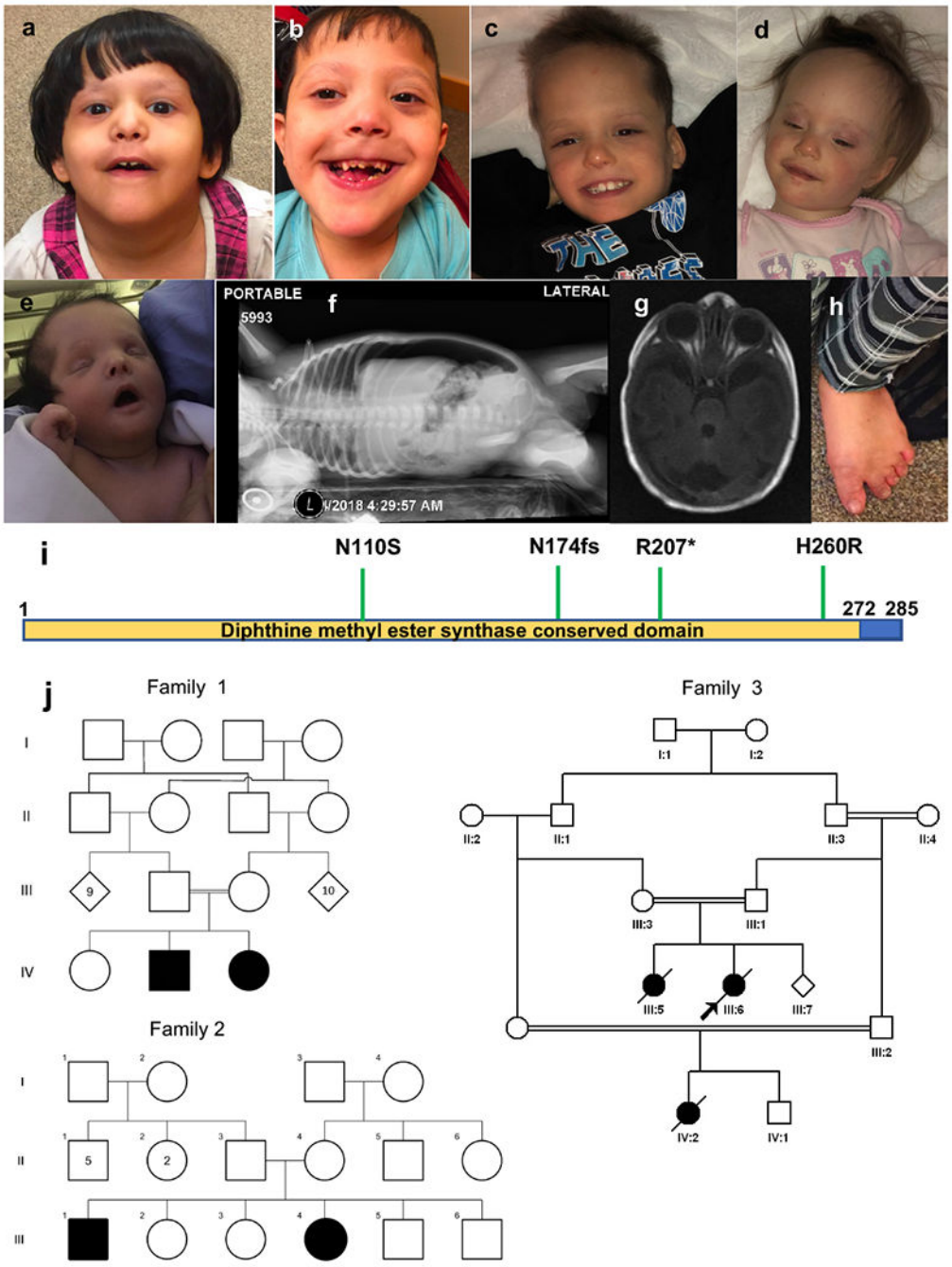

Figure 1. Clinical features of individuals with *DPH5* variants.

A., B. Siblings from family 1. C., D. Siblings from family 2. E-G. Proband from family 3. Craniofacial appearance, including sparse hair and eyebrows, broad forehead with frontal bossing, epicanthal folds, broad nasal bridge, upturned nasal tip, and triangular chin, seen in all individuals; down turned corners of the mouth seen in individuals (A) and (E). B. Poor dentition. F. Chest and abdominal X-ray with pneumoperitoneum owing to perforated bowel. G. Axial view of head computed tomography showing bilateral minimal tentorial subdural hemorrhage and enlarged cisterna magna. H. Brachydactyly of toes for individual (B) from

family 1. I. Schematic of DPH5 protein showing that all variants identified in the 3 families fall within the conserved domain diphthine methyl ester synthase. J. Family pedigrees of 3 families harboring *DPH5* variants. Pedigree 1 is for family 1 with 2 affected siblings born to a consanguineous family from Syria. Pedigree 2 is for family 2 with 2 affected siblings of European ancestry from Boston. Pedigree 3 is for family 3 from Saudi Arabia showing additional affected sibling and an affected first cousin.

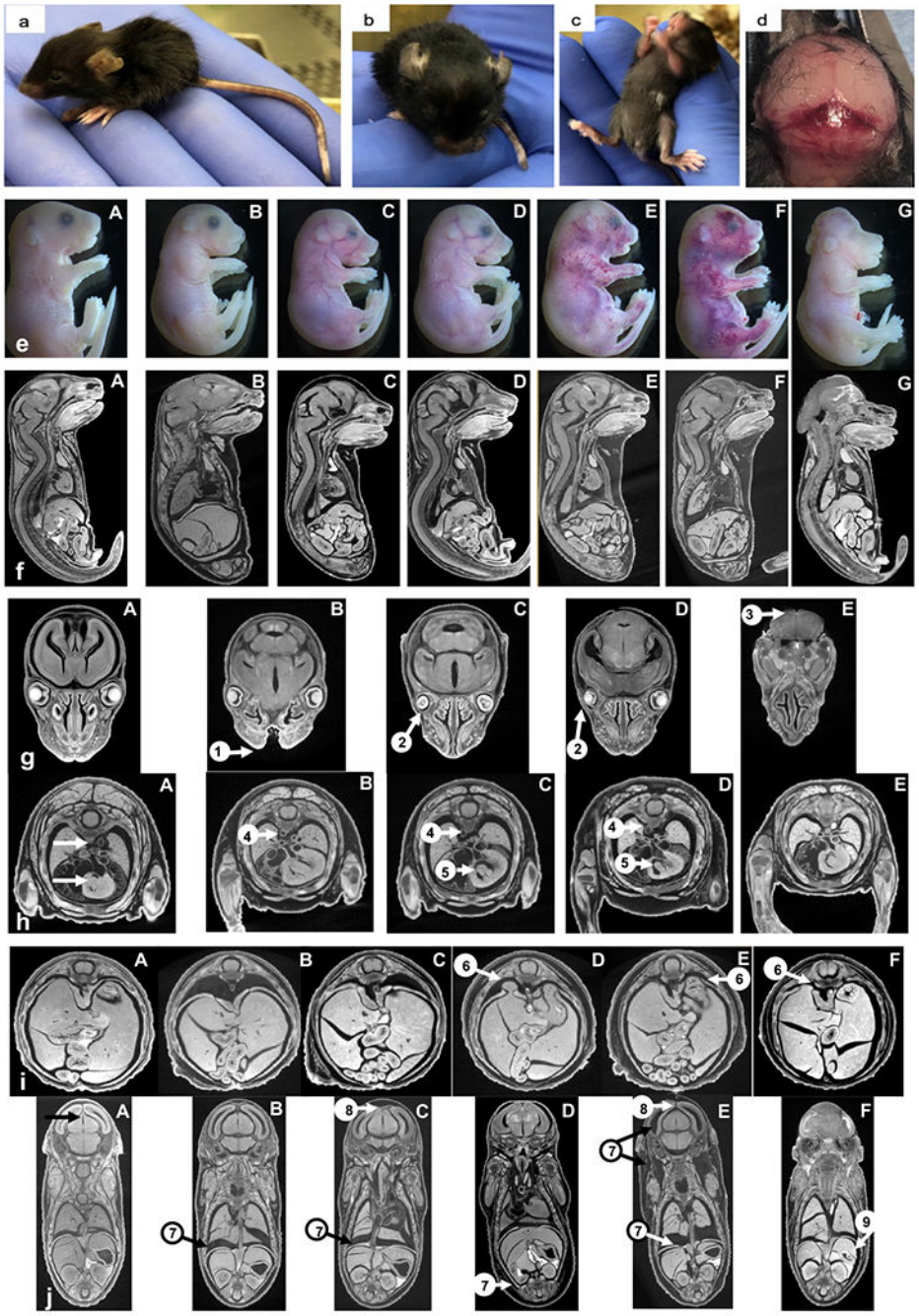

Figure 2. Images of prenatal and postnatal homozygous *Dph5* mice.

A-C. Homozygous female *Dph5*_pH260R mouse aged at 21 days presenting with decreased body size, dysmorphic head morphology, depigmented patch on abdomen, and polydactyly of left hind foot. D. Postmortem photo at age 24 days with observed hemorrhage around the lambdoid skull sutures. E., F. Photomicrographs of embryonic day (ED) 18.5(1) Wild type (WT) and (2-7) homozygous *Dph5* embryos with their corresponding micro computed tomography (μCT) images (sagittal sections) showing: (4, 7) facial clefts, (7) exencephaly, (5,6) microphthalmia, (7) anophthalmia, (4-6) shortened frontonasal prominence, and (5,6)

vascular hemorrhage with edema. G., H. μCT images (transverse sections) of ED 18.5 (1) WT and (2, 4, 6, 7) homozygous *Dph5* embryos through (7) head and (8) heart showing facial cleft (arrow i), microphthalmia (arrow ii), anophthalmia with exencephaly (arrow iii), situs inversus of the dorsal aorta (arrow iv) (and arch aorta, not shown), and ventricular septal defects (arrow v). Arrows in(H, 1) WT show normal position of dorsal aorta and closed heart interventricular septum. I., J. μCT images of visceral cavity (transverse section), and frontal sections of (1) WT and (2-6) homozygous embryos showing diaphragmatic hernia (arrow vi), edema in pleural cavity, lymphatic sacs, brain vesicles and trunk (arrow vii), hypoplastic/absent pineal gland (arrow viii), and hypoplastic stomach (arrow ix).

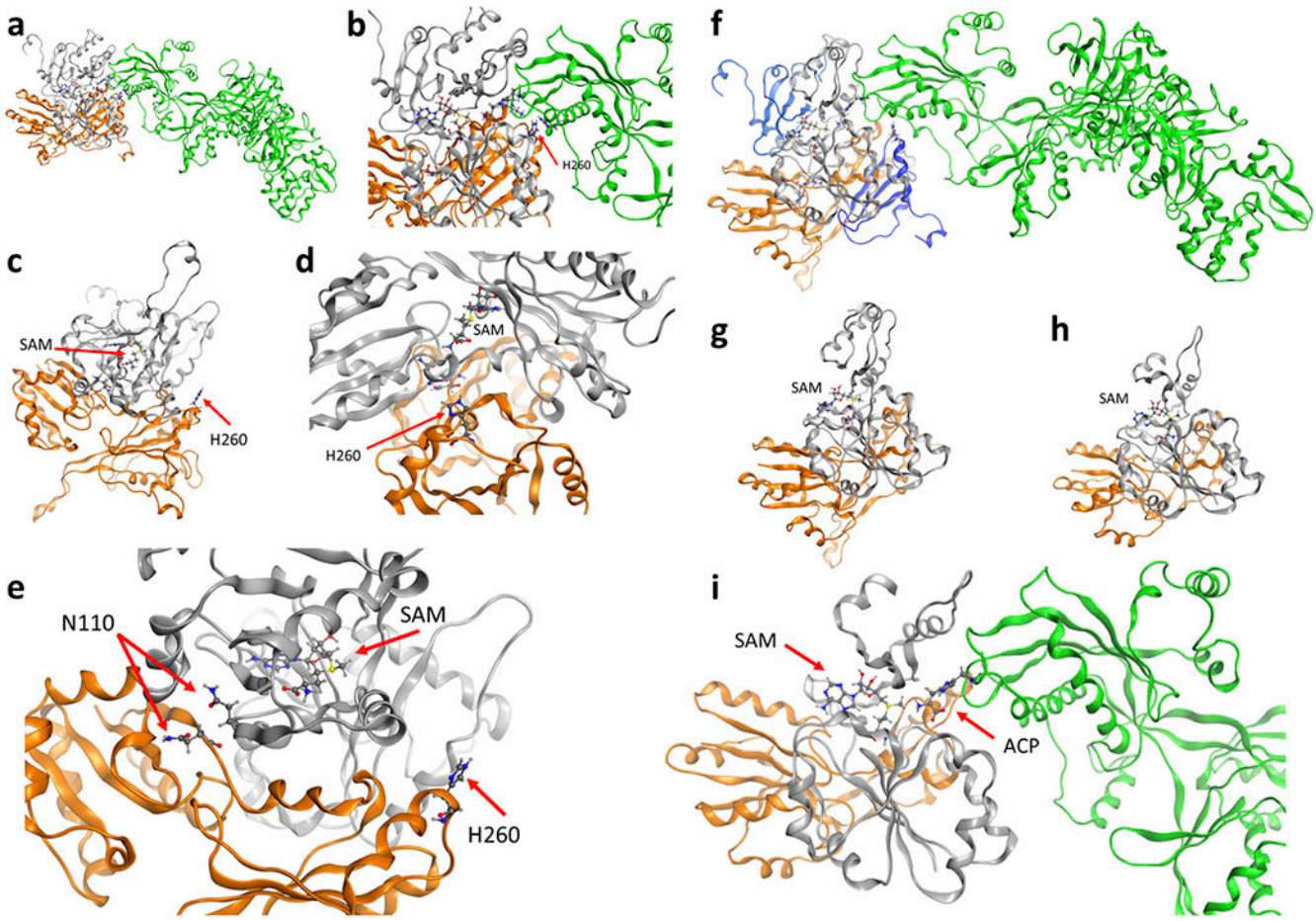

Figure 3. Homology models of wild type (WT), p.His260Arg, p.Asn110Ser, p Arg207Ter, and p.Asn174LysfsTer10 variants of human *DPH5* and interaction with eEF2.

A. Human WT *DPH5* dimer (gray/golden) in complex with eEF2 model (green). B. Zoomed image of (A), p.His260 interacts favorably with p.Arg711 and p.Lys582 of eEF2. In yeast DPH5, p.His260 corresponds to p.His257, interacting in the same way with eEF2.16. C., D. p.His260Arg homology modeling fold is identical to the WT. p.Arg260 will be positioned at the protein interface interacting with eEF2. In the *S cervisae* system, the corresponding residue interacts with p.Arg711 and p.Lys582 of eEF2; the p.His260Arg variant will introduce repulsion owing to its positive charge and weakened protein–protein interaction. C. Sideview (eEF2 interacting from the right; not shown). D. Rotated (90°) zoom-in facing the interaction region binding to eEF2. E. p.Asn110 is located at the DPH5 monomer–monomer interface region. p.Asn110Ser variant may weaken the dimer stability and thus lead to malfunctioning DPH5-eEF2 interaction. It is also possible that exchange of SAM (as eEF2 is methylated 4 times by DPH5) is impaired by the variant. F., G. p.Arg207Ter truncation variant. F. This truncation will remove a large part of the region interacting with eEF2, including p.His260 (dark blue showing the truncated parts of monomer 1), as well as SAM binding (light blue showing the truncated part of monomer 2). It can thus be expected that DPH5–eEF2 interaction as well as DPH5 functionality is severely disrupted. G. DPH5 truncated at p.Arg207, showing the exposed SAM and the much smaller area of interaction

toward eEF2. H., I. The p.Asn174LysfsTer10 introduces a stop codon after p.Leu182 in the p.Asn174LysfsTer10 variant, leading to premature truncation and reduced area of interaction with eEF2. I. The interaction between the p.Asn174LysfsTer10 variant DPH5 and eEF2 is significantly reduced, and SAM is largely solvent exposed. ACP, 3-amino-3carboxypropyl; SAM, S-adenosyl methionine.

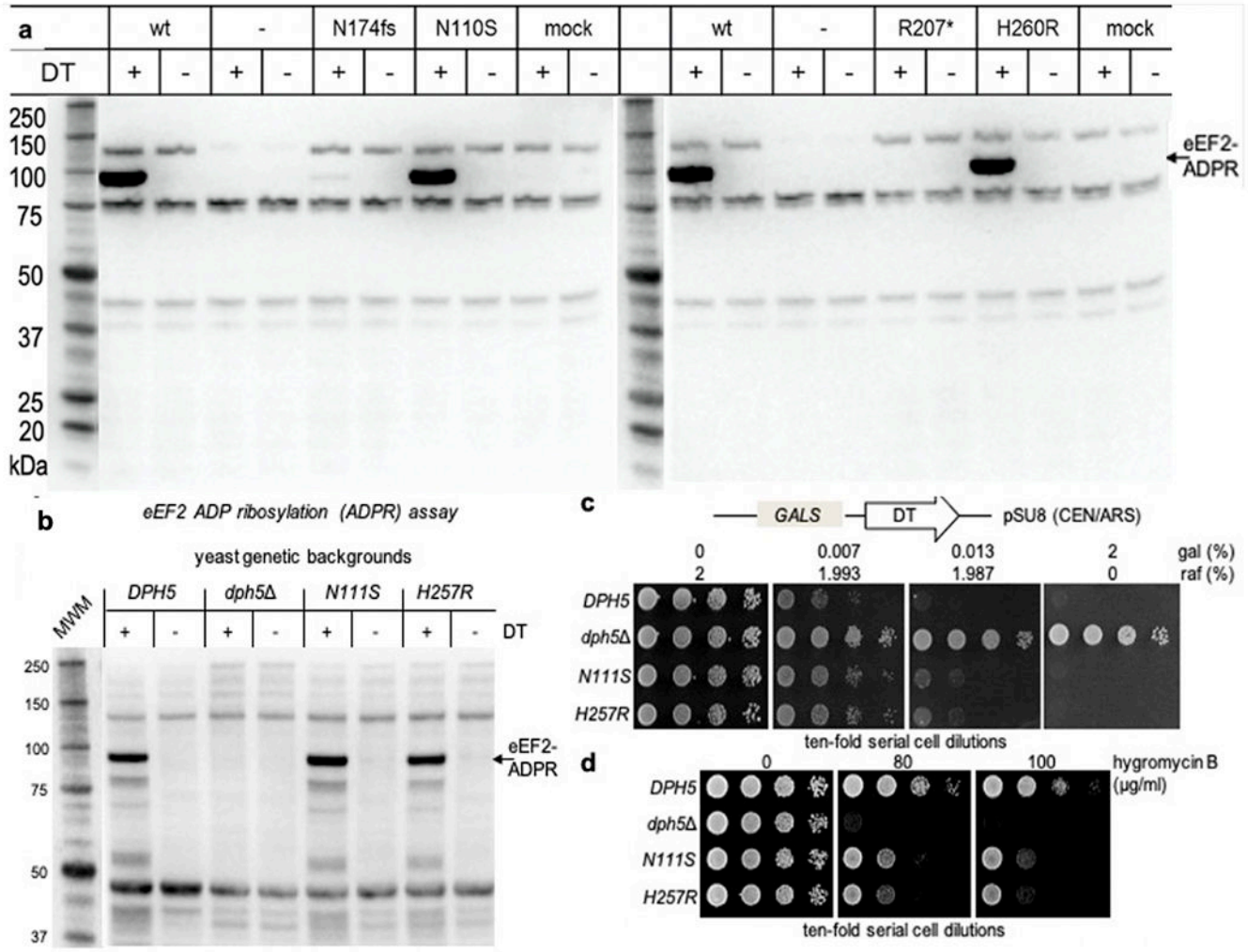

Figure 4. XXX.

A. ADPR assays indicate loss of function of *DPH5* p.Arg207Ter and p.Asn174LysfsTer10. Radioimmunoprecipitation assay extracts of MCF7 DPH5-knockout (KO) cells[27] transfected with expression plasmids encoding *DPH5* WT, p.Asn174LysfsTer10, p.Asn110Ser, p.Arg207Ter, and p.His260Arg were incubated with DT and biotinylated nicotinamide adenine dinucleotide (Bio-NAD) to assess the presence or absence of diphthamide. Successful ADPR with Bio-NAD as substrate generates biotinylated eEF2, which can be detected in sodium dodecyl sulfate–polyacrylamide gel electrophoresis blots probed with streptavidin-horseradish peroxidase and peroxidase substrate. Presence of diphthamide (generated by recombinant *DPH5* in the *DPH5*-KO background) therefore produces a band at approximately 100 kDa and is seen with WT, p.Asn110Ser, and p.His260Arg. Reactions without DT and extracts of nontransfected or mock-transfected cells serve as controls. B-D. Assays diagnostic for yeast diphthamide modification capacity in vivo. B. ADPR assay with total protein extracts of yeast BY4741 strains WT (*DPH5*), *dph5Δ*, p.Asn111Ser, and p.His257Arg. Extracts were incubated with DT and Bio-NAD to assess the presence or absence of diphthamide. Presence of diphthamide results in successful ADPR and produces a band at approximately 100 kDa as seen with WT and p.Asn111Ser

and p.His257Arg variants. Reactions without DT serve as controls. C. Phenotypic spot assay investigating growth inhibition by the diphthamide-dependent DT. Cells carrying the galactose inducible DT expression vector pSU8[31] were 10-fold serially diluted and cultivated on medium containing the indicated concentrations (%[weight/volume]) of raf and/or gal at 30 °C for 3 days. Cells with the 2 variants p.Asn111Ser and p.His257Arg exhibited higher tolerance to DT than WT but much less than the cells with *dph5Δ*. D. Assay displaying sensitivity to diphthamide-indicative translation inhibitor drug hygromycin B[18] was examined by cultivation on medium containing the indicated doses of hygromycin B at 30 °C for 2 days. Cells with the p.Asn111Ser and p.His257Arg variants were more sensitive to hygromycin than WT cells but less sensitive than cells with *dph5Δ*. ADPR, adenosine diphosphate-ribosylation; DT, diphtheria toxin; gal, galatose; raf, raffinose; WT, wild type.

Table 1:

Molecular and phenotypic characteristics of five individuals from three families with *DPH5* (NM_001077394.2) variants.

Features	Family 1 A	Family 1 B	Family 2 A	Family 2 B	Family 3 A
Genetic variant	**c.779A>G Homozygous**	**c.779A>G Homozygous**	**c.619C>T; c.329A>G Heterozygous**	**c.619C>T; c.329A>G Heterozygous**	**c.521dupA Homozygous**
Protein Change	**p.His260Arg**	**p.His260Arg**	**p.Arg207*; p.Asn110Ser**	**p.Arg207*; p.Asn110Ser**	**p.Asn174LysfsTer10**
Age	10 years	8 years	9 years	1 year	11 days
Sex	Female	Male	Male	Female	Female
Height	Z=−2.5 SD	Z= −1.18	Z=−4.99 SD	Z= −3.06 SD	NA
Weight	FTT initially now 10th percentile with G tube feeds	27 kg (70th percentile)	5 SD below mean	3.45 SD below mean	BW 800 Gms
Head circumference	50.5 cms (14th percentile)	51 cms (23rd percentile)	51.5 cm (13th percentile)	42 cm (32nd percentile)	NA
Facial features	Broad forehead, bitemporal narrowing, sparse eyebrows, epicanthal folds, deep set eyes, broad nasal bridge, rounded tip of nose, downturned corners of mouth, high arched palate, triangular chin, dental carries	Broad forehead, bitemporal narrowing sparse eyebrows, epicanthal folds, wide palpebral fissures, broad nasal bridge, rounded nasal tip, downturned corners of mouth, triangular chin, multiple dental caries	High forehead, high anterior hairline, depressed midface, upslanting eyes, sparse eyelashes, mild epicanthal folds, thick alveolar ridges	Prominent forehead, depressed midface, broad alveolar ridges, faint eyebrows, upslanting eyes	Broad forehead, bitemporal narrowing sparse eyebrows, epicanthal folds, wide palpebral fissures, deep set eyes, broad nasal bridge, rounded nasal tip, downturned corners of mouth triangular chin, micrognathia
Prenatal/birth history	Decreased fetal movement in pregnancy, born at 42 weeks	Normal pregnancy, NSVD	Decreased fetal movement, excess fluid at delivery	Excess fluid at delivery	Polyhydramnios. Preterm baby was delivered via CS due to breech presentation
Postnatal	NICU stay for hypoxia - 2 days	No issues	Hospital stay for 3 weeks for poor feeding	No issues	Cyanosis
Developmental delays	Global	Global	Global	Global	NA
Motor	Limited walking, smiles, clap hands, crawls, cruises and walks household distances independently	Crawling	Not walking	Very delayed	NA
Speech and language	Nonverbal	Nonverbal	Nonverbal	Nonverbal	NA
Intellectual disability	Yes, profound	Yes, profound	Yes, profound	Yes	NA
Behavioral concerns	Screaming episodes	Happy disposition	NA	NA	NA
CNS	Congenital hypotonia, cerebral palsy, sleep difficulties,	Seizures, spastic quadriplegia, cerebral palsy, contractures, weakness, DTRs 3+, plantars upgoing	Seizure, appendicular spasticity, central hypotonia, regression in motor skills	Myoclonic seizures, central hypotonia, appendicular hypertonia	Congenital hypotonia
Brain Imaging studies	Brain atrophy (by report on MRI at 1 yo) CT scan at 8 yo normal	Normal at age 5 yo	Focal lesion in white matter of left inferior frontal gyrus, vertically oriented	Diffuse paucity of white matter, cerebellar vermian hypoplasia	“Strawberry head” by ultrasound, MRI Bilateral minimal tentorial subdural hemorrhage and enlarged cisterna magna

Features	Family 1 A	Family 1 B	Family 2 A	Family 2 B	Family 3 A
			hippocampi, prominence of ventricular system		
EEG	Abnormal -continuous slowing consistent with mild to moderate encephalopathy	Abnormal, consistent with generalized disturbance of cerebral function with multifocal epileptogenic brain abnormality	Abnormal	Abnormal, consistent with epileptic myoclonus	NA
Ocular findings and Vision	Fixes and follows	Ocular melanocytosis, pathological high myopia −11DS, fixes and follows	Gray sclera with ocular melanocytosis, strabismus requiring surgery	Gray sclera, cortical visual impairment	NA
Hearing	Normal	Normal	Normal	Normal	NA
Audiology	ABR Normal	ABR Normal	NA	NA	NA
CVS	Trivial mitral prolapse & regurgitation, EKG normal	Trivial mitral prolapse & regurgitation, EKG: sinus tachycardia	Congenital aortic dilatation	Aortic dilatation	Multiple muscular VSD and ASD, hypoplastic pulmonary artery, pericardial effusion
RS	Normal	Dyspnea, obstructive sleep apnea, asthma, recurrent aspiration, pneumonia, dependent on oxygen therapy at night	Breath-holding spells	Normal	Normal
GI	Feeding difficulties, dysphagia, GJ-tube fed, bowel incontinence	GJ-tube dependent, hematemesis	G-tube	GERD	Extensive pneumoperitoneum Day 10 postnatal emergency surgery for bowel perforation , died following day at 11 days of life
Endocrinology	Short stature	Short stature	Short stature	Short stature	NA
Musculoskeletal	Lean muscle mass, small hands and feet, tapered fingers, brachydactyly of 3rd toe bilateral	Lean muscle mass, tapered fingers, pes planus, Bracydactyly of 4 toes other than big toe bilateral	Rocker bottom feet, hyperextensible joints, tapered fingers, right single crease, small hands and feet	Tapered fingers	NA
Genitourinary	Urinary incontinence	Urinary incontinence	No known issues	No known issues	NA
Dermatology	Normal	Normal	Extensible skin	Extensible skin, pale	NA
Significant Family history	One previous live birth with mortality at week of age; Similarly affected sibling, 1 B in this study	One previous live birth with mortality at 1 week of age; Similarly affected sibling, 1 A in this study	Similarly affected sibling, 2B in this study	Similarly affected sibling, 2A in this study	Multiple spontaneous miscarriages, one antepartum stillbirth and a neonatal death. The two deceased babies had microphthalmia, hypertelorism, IUGR, TOF, hydrocephalus and cerebellar hypoplasia

Abbreviations: *ABR* auditory brain response, *CNS* central nervous system, *CVS* cardiovascular system, *DS* diopter spherical, *RS* respiratory system, *EEG* electroencephalogram, *EKG* electrocardiogram, *FTT* failure to thrive, *GERD* gastroesophageal reflux disease, *GI* gastrointestinal, *IUGR* intrauterine growth retardation, *NA* not available, *TOF* tetralogy of Fallot